

# Structural disorder in the $\text{Pb}_2\text{Sr}_2\text{Y}_{1-x}\text{Ca}_x\text{Cu}_3\text{O}_{8+\delta}$ cuprates

U. Staub

*Swiss Light Source Project, Paul Scherrer Institute, CH-5232 Villigen PSI, Switzerland*

L. Soderholm and S. Skanthakumar

*Chemistry Division, Argonne National Laboratory, Argonne, Illinois 60439*

P. Pattison

*Institut de Crystallographie, Université de Lausanne, CH-1015 Lausanne, Switzerland*

K. Conder

*Laboratorium für Festkörperphysik, Eidgenössische Technische Hochschule, CH-8093 Zürich, Switzerland*

(Received 15 July 1997; revised manuscript received 10 September 1997)

High-resolution powder x-ray-diffraction results on  $\text{Pb}_2\text{Sr}_2\text{Y}_{1-x}\text{Ca}_x\text{Cu}_3\text{O}_{8+\delta}$  are presented. Assuming an orthorhombic cell with  $Cmmm$  symmetry, the reflections that index with  $h$  and  $l$  simultaneous nonzero are observed to be distinctly broader than the other reflections. A model is presented that is able to explain quantitatively and qualitatively the relative widths of the different  $hkl$  reflections. The widths of the reflections are found to be independent of the doping level. The model employed is based on anisotropic distributions of the  $d$  spacings within the  $(a,c)$  plane, corresponding to a fluctuation of the  $\beta$  angle around  $90^\circ$  that occurs as a result of oxygen nonstoichiometry. The distortions may be related to the incommensurate modulation along the  $b$  direction in the structurally similar  $(\text{Bi/Pb})_2\text{Sr}_2(\text{Ca/Y})\text{Cu}_2\text{O}_{8+\delta}$  compounds. At elevated temperatures, a disorder-order phase transition ( $T_{\text{do}}=240^\circ\text{C}$ ) is observed. At temperatures above  $T_{\text{do}}$ , the structure relaxes to the undistorted average orthorhombic structure. This order-disorder transition results from oxygen diffusion, which sets in at the transition temperature. [S0163-1829(98)02909-9]

## I. INTRODUCTION

It is well known that the structures of perovskite-based high- $T_c$  superconductors inherently contain a variety of defects (see, e.g., Ref. 1). Many of these defects are induced by the nonstoichiometry that often occurs in these compounds. In particular, additional oxygen ions or oxygen vacancies induce distortions that can either order, as exemplified by the ortho-II phase in the  $\text{RBa}_2\text{Cu}_3\text{O}_{6+x}$  series,<sup>2</sup> or can be disordered as in the  $\text{R}_{2-x}\text{Ce}_x\text{CuO}_{4-\delta}$  series.<sup>3</sup> The superconducting properties are extremely sensitive to these types of distortions. Changes in the concentration of vacancies may lead to structural and electronic phase transitions as for  $x \approx 0.4$  in the  $\text{RBa}_2\text{Cu}_3\text{O}_{6+x}$  series. The  $(\text{Bi}_{1-x}\text{Pb}_x)_2\text{Sr}_2(\text{Ca/Y})\text{Cu}_2\text{O}_{8+\delta}$  compounds crystallize with incommensurate modulations to the chemical structure that occur in the  $b$  direction. These modulations depend on  $x$ , the relative  $\text{Bi}^{3+}$  to  $\text{Pb}^{2+}$  concentration,<sup>4</sup> and they are believed to be induced in part by distortions due to oxygen vacancies.<sup>5</sup> It is argued that additional oxygen ions compensate for the lattice mismatch between the  $\text{BiO}$  and the perovskite layers.<sup>4</sup> A different type of defect was found in the  $\text{R}_2\text{Ba}_4\text{Cu}_7\text{O}_{14+x}$  series, in which stacking faults along the  $c$  direction were reported.<sup>6</sup> Also the magnetic structure of the rare-earth sublattice in  $\text{RBa}_2\text{Cu}_3\text{O}_{7-\delta}$  [ $\text{R}=\text{Ho}$  (Ref. 7) and  $\text{Nd}$  (Ref. 8)] and in  $\text{Pb}_2\text{Sr}_2\text{Tb}_{1-x}\text{Ca}_x\text{Cu}_3\text{O}_{8+\delta}$  (Ref. 9) have been found to exhibit stacking faults consistent with finite correlation lengths along the  $c$  direction.

Recently, there has been interest in studying the effects of substituting selected rare earths ( $\text{R}=\text{Ce}$ ,  $\text{Pr}$ , and  $\text{Tb}$ ) into the

$\text{Pb}_2\text{Sr}_2\text{R}_{1-x}\text{Ca}_x\text{Cu}_3\text{O}_{8+\delta}$  (2213) series, and comparing the results with similar substitutions into the  $\text{RBa}_2\text{Cu}_3\text{O}_{7-x}$  series. There are significant differences in the chemical and electronic properties of these  $\text{R}$  substitutions into the two different hosts. In particular, the magnetic and electronic properties of the  $\text{R}$  ion were studied by different techniques.<sup>9-14</sup> The parent  $\text{Pb}_2\text{Sr}_2\text{RCu}_3\text{O}_{8+\delta}$  are made superconducting by replacing some  $\text{R}^{3+}$  by either vacancies or  $\text{Ca}^{2+}$ .<sup>15,16</sup> The structure of the  $\text{Y}$  analog has been previously reported as monoclinic ( $C2/m$ ,  $P2_1/m$ , or  $P2_1$ ) (Refs. 16 and 17) or orthorhombic ( $Cmmm$ ,  $Pmm$ ,  $Pmmm$ ).<sup>17-21</sup> Neutron-diffraction data obtained from  $\text{Pb}_2\text{Sr}_2(\text{R/Ca})\text{Cu}_3\text{O}_{8+\delta}$  ( $\text{R}=\text{Tb}$ ,  $\text{Y}$ ,  $\text{Pr}$ , and  $\text{Ce}$ ) were fit using the  $Cmmm$  space group,<sup>11</sup> despite the presence of extra reflections that violate the  $C$  centering, and the presence of a subset of significantly broadened reflections. The extra reflections, with  $hkl$  indices of type  $h+k$  odd, are very weak. These extra reflections have been previously observed,<sup>22-24</sup> and have been used to fit a cell with  $Pmmm$  symmetry. Unfortunately, the limited number of extra reflections, combined with their very weak intensity, severely limits any attempt to fit the data to a symmetry lower than  $Cmmm$ .<sup>22</sup> The broadening of selected reflections may also indicate splittings associated with a symmetry lower than orthorhombic, but the broadened peaks could not be resolved into multiple components due to the limited experimental resolution available in these studies. Similar broadening of particular  $hkl$  reflections were also observed in  $\text{Pb}_2\text{Sr}_2\text{YCu}_3\text{O}_{8+\delta}$  by powder x-ray diffraction<sup>25</sup> and were interpreted in terms of stacking faults along the  $c$

direction. It has been shown that the  $hkl$ -dependent broadening disappears at elevated temperatures (473 K), which would consequently indicate a phase transition from monoclinic to orthorhombic.<sup>11</sup> However, the intensities of the weak extra reflections have been found to be temperature-independent. In addition, a recent neutron-diffraction study on the magnetic ordering of the  $\text{Tb}^{3+}$  sublattice at low temperature in  $\text{Pb}_2\text{Sr}_2\text{TbCu}_3\text{O}_{8+\delta}$  found similar broadened reflections associated with the long-range 3-dimensional spin phase.<sup>9</sup> However, no consistent picture about the structure, which could also explain the  $hkl$ -dependent broadening has emerged yet.

Herein we present a high-resolution, powder x-ray-diffraction study of  $\text{Pb}_2\text{Sr}_2\text{Y}_{1-x}\text{Ca}_x\text{Cu}_3\text{O}_{8+\delta}$  ( $x=0$  and  $x=0.5$ ). We find that all reflections  $hkl$  with  $h$  and  $l$  simultaneously nonzero are broadened compared to the other lines. The excellent angular and energy resolution obtainable with high brilliant Synchrotron radiation permits us to show that the broadening is intrinsic and cannot be described as a simple splitting of the peaks. These data show that the broadening of selected reflections is the result of lattice distortions that lead to a distribution in the  $d$  spacings that cannot be well described in a symmetry lower than orthorhombic. We present a model that describes this behavior both quantitatively and qualitatively as distortions in the  $a$ - $c$  plane. Further data, obtained as a function of increasing temperature, show that the widths of the broadened reflections start to decrease at about 180 °C, and have narrowed at 300 °C, indicating a disorder-order phase transition ( $T_{\text{do}} \approx 240$  °C). It is shown that this disorder-order phase transition is connected with the mobility of the nonstoichiometric oxygen ions above 200 °C.

## II. EXPERIMENTS

Polycrystalline  $\text{Pb}_2\text{Sr}_2\text{Y}_{1-x}\text{Ca}_x\text{Cu}_3\text{O}_{8+\delta}$  ( $x=0$  and  $0.5$ ) samples were prepared by first weighting out stoichiometric amounts of  $\text{PbO}$ ,  $\text{Y}_2\text{O}_3$ ,  $\text{CuO}$ ,  $\text{CaO}$ , and  $\text{SrCO}_3$ , followed by an intimate mixing in an agate mill, pelletizing and sintering at 830 °C for 20 h in an argon/oxygen mixture of 98%/2%. After furnace cooling to room temperature, we checked the samples with x-ray diffraction. Milling, pelletizing, and sintering under pure argon atmosphere were repeated until the x-ray-diffraction patterns verified the single phase character of the samples, except for the  $x=0.5$  compound where some small amount of impurity phases were detected. The superconducting transition temperature ( $T_c = 70$  K) of the  $x=0.5$  compound was determined by measuring the magnetization as a function of temperature with a commercial superconducting quantum interference device.

The high-resolution x-ray-diffraction experiments were performed at the Swiss Norwegian Beamline BM1 at the European Synchrotron Radiation Facility in Grenoble, France. Extended diffraction Debye patterns were collected in standard Scherrer geometry with a wavelength of  $\lambda = 1.1$  Å at room temperature. The angular resolution in  $2\theta$  was about 0.03°. For certain reflections and for the patterns obtained at elevated temperatures, a Si (111) analyzer crystal was installed in order to improve the  $2\theta$  resolution to 0.01°. A gas-stream furnace was installed to heat the sample up to 500 °C. The temperature was controlled by two thermo-

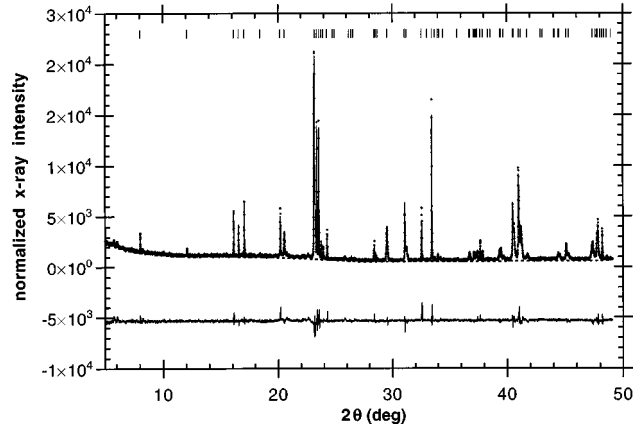


FIG. 1. High-resolution x-ray-diffraction pattern, Rietveld fit, and residual of  $\text{Pb}_2\text{Sr}_2\text{YCu}_3\text{O}_{8+\delta}$  taken at room temperature and with  $\lambda = 1.1$  Å.

couples located just below the sample and the x-ray beam. The experiments under improved resolution were performed with  $\lambda = 1$  Å, which corresponds to an energy just below the  $L_3$  edge of lead. The samples were sealed in a 0.5 mm diameter quartz capillary.

## III. RESULTS

The diffraction pattern obtained at room temperature of the parent, nonsuperconducting  $\text{Pb}_2\text{Sr}_2\text{YCu}_3\text{O}_{8+\delta}$  compound is shown in Fig. 1. As mentioned above, the peaks can be indexed using an orthorhombic cell with parameters  $a = 5.3943$ ,  $b = 5.4337$ , and  $c = 15.7251$ . Assuming this cell for indexing the reflections, Figs. 2(a) and 2(b) show two regions with enlarged  $2\theta$  scale showing the 114, 020, and 200 (a) as well as the 025 and the 205 reflections (b). The width of all observed reflections, measured under improved resolution conditions, are broader than the instrumental resolution in all three crystallographic directions. All reflections with  $h$  and  $l$  indices simultaneously nonzero are broader than the other peaks, as exemplified by the 114 and the 205 reflections, which are distinctly broader than the other peaks. We note that the width of the  $00l$  reflections slightly increases upon increasing value of  $l$  as shown in Fig. 3. However, the broadening of these peaks is distinctly smaller than those of  $h0l$  type. The increased width of these reflections, over that expected from the instrument resolution, clearly indicates that their broadening is not the result of unresolved splittings caused by a lowering in symmetry. Instead, the broadening is interpreted as a distribution of  $d$  spacings along certain crystallographic directions. The full width at half maximum  $\Gamma$  for a selected number of well-resolved reflections for  $\text{Pb}_2\text{Sr}_2\text{YCu}_3\text{O}_{8+\delta}$  is shown in Fig. 4. The  $hkl$  dependence of  $\Gamma$  for the superconducting  $x=0.5$  and the parent  $x=0$  compound was found to be very similar.

In order to describe the selected-line broadening in the  $\text{Pb}_2\text{Sr}_2\text{Y}_{1-x}\text{Ca}_x\text{Cu}_3\text{O}_{8+\delta}$  compounds, an approach was used that is similar to that used to describe the orthorhombic strain in  $\text{La}_2\text{NiO}_4$ .<sup>26</sup> The linewidth can be interpreted as a Gaussian distribution of  $d$  spacings. The relevant variable for an interpretation of the diffraction pattern is the squared inverse of the lattice spacing, which is a function of the mean values of

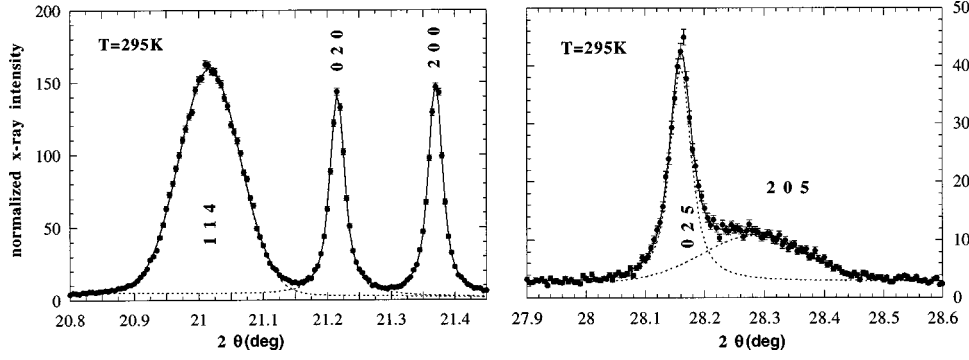


FIG. 2. (a) and (b) Selected regions of x-ray-diffraction patterns of  $\text{Pb}_2\text{Sr}_2\text{YCu}_3\text{O}_{8+\delta}$  taken at room temperature using improved resolution (Si 111 analyzer). The full line corresponds to the total fit to Voigtians and the dotted line to the subdivision into the different reflections.

the lattice constants. The variance of  $1/d_{hkl}^2$  can be expressed as

$$\sigma^2(1/d_{hkl}^2) = \sum_i \sum_j S_{ij} \frac{\partial(1/d_{hkl}^2)}{\partial \alpha_i} \frac{\partial(1/d_{hkl}^2)}{\partial \alpha_j}, \quad (1)$$

where  $\alpha_i$  corresponds to the lattice constants  $a$ ,  $b$ , and  $c$  and unit-cell angles  $\alpha$ ,  $\beta$ ,  $\gamma$ , and  $S_{ij}$  to a covariance matrix. Assuming that the peak broadening of the lattice spacing fluctuations is Gaussian, the broadening produced by the sample and the broadening from the instrumental resolution add in quadrature to produced the square of the observed peak width,  $\Gamma$ . Therefore, the  $\Gamma$  of the  $hkl$  reflections can be given by a modified Cagliotti expression as

$$\Gamma^2(2\theta) = (U+T)\tan^2 \theta + V \tan \theta + W \quad (2)$$

with

$$T = 8 \ln 2 [d_{hkl}^4 \sigma^2(1/d_{hkl}^2)]. \quad (3)$$

The fact that  $hkl$  reflections with simultaneous  $h$  and  $l$  non-zero are significantly broadened is reflected in the fact that either  $S_{13}$  or  $S_\beta$  ( $S_{55}$ ) is the dominant term in the correlation matrix. The slight  $l$  dependence of  $\Gamma$  of the  $00l$  reflections indicate a small  $S_{33}$  term, in addition to an isotropic strain term which leads to  $hkl$ -independent broadening of the reflections. For average orthorhombic symmetry ( $\beta=90^\circ$ ) fluctuations of the local monoclinic angle  $\beta'$  and the  $c$  axis can be described by transforming Eq. (1) for the variance of  $(1/d_{hkl}^2)$  into

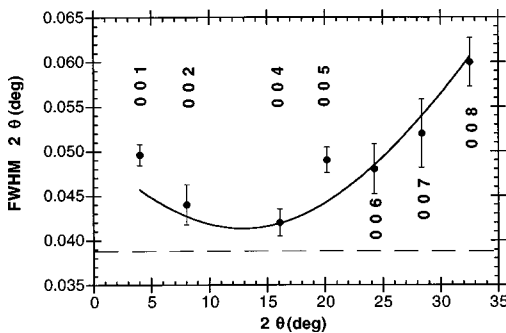


FIG. 3.  $2\theta$  dependence of the half-widths for 00l type of reflections. The line corresponds to the fit with  $S_{33}$  term only. The broken line corresponds to the isotropic broadening of the reflection (e.g., 020 or 200).

$$\begin{aligned} \sigma^2 &= S_\beta \left[ \frac{\partial(1/d_{hkl}^2)}{\partial \beta} \right]_{\beta=90^\circ}^2 + S_{33} \left[ \frac{\partial(1/d_{hkl}^2)}{\partial c} \right]^2 \\ &= S_\beta \frac{4h^2l^2}{a^2c^2} + S_{33} \frac{4l^4}{c^6}. \end{aligned} \quad (4)$$

We note that essentially the same result is obtained using an  $S_{13}$  term. However,  $S_{13}$  describes the correlation between the lattice fluctuations in the  $a$  and  $c$  direction implying relevant contributions in those directions, which is not supported by the experimental data.

The values obtained by fitting this model to the  $\Gamma$  determined from the data (Fig. 4) are listed in Table I. The values found for  $x=0$  and 0.5 are different outside their error limits. However, a comparison with samples from other batches indicates that the differences are likely to come from slightly different oxygen contents and not from Ca doping. By inserting this description for the  $hkl$  dependence of the width into the Rietveld refinement program FULLPROF,<sup>27</sup> we were able to obtain a satisfactory description of the observed diffraction pattern using the orthorhombic space group Cmmm (see Fig. 1). We note that the strong absorption of the sample did not permit a reliable determination of the Debye-Waller factors and the atomic position parameters. To obtain those, the

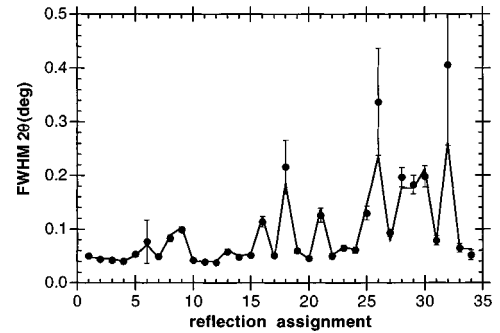


FIG. 4. Half widths for a selected number of reflections. The line corresponds to the fit with a covariance matrix with  $S_\beta = 0.071 \pm 0.003$  and  $S_{33} = 0.20 \pm 0.05$ . (1=001, 2=002, 3=004, 4=110, 5=111, 6=112, 7=005, 8=113, 9=114, 10=020, 11=200, 12=021, 13=201, 14=006, 15=007, 16=116, 17=025, 18=205, 19=008, 20=220, 21=118, 22=131, 23=311, 24=028, 25=119, 26=208, 27=134, 28=314, 29=226, 30=228, 31=0210, 32=2010, 33=040, 34=400).

TABLE I. Lattice constants and covariance matrix elements determined from  $\text{Pb}_2\text{Sr}_2\text{Y}_{1-x}\text{Ca}_x\text{Cu}_3\text{O}_{8+\delta}$  at room temperature using the model described in the text.

	$x=0$	$x=0.5$
$a$ (Å)	5.3935(1)	5.3790(3)
$b$ (Å)	5.4320(1)	5.4188(3)
$c$ (Å)	15.7146(3)	15.7371(8)
$S_\beta$	0.071 (3)	0.082 (4)
$S_{33}$	0.20 (5)	0.4 (1)
$(S_{13})$	5.6 (2)	7.2 (4)

analysis applied herein should be performed on high-resolution neutron-diffraction data.

Figure 5 shows the 025 and 205 reflections as a function of temperature. The 205 peak is distinctly narrower at 245 °C and it has the same width as the 025 reflection at 300 °C. The same narrowing of the peaks is observed for all the reflections with  $h$  and  $l$  simultaneously nonzero. However, all the observed peaks remain broader than expected from the instrumental resolution alone, indicating that there remains an isotropic distribution in the lattice spacing.

Figure 6 shows the temperature dependence of the width  $\Gamma$  and the position of the 114 reflection. Whereas  $\Gamma$  is almost

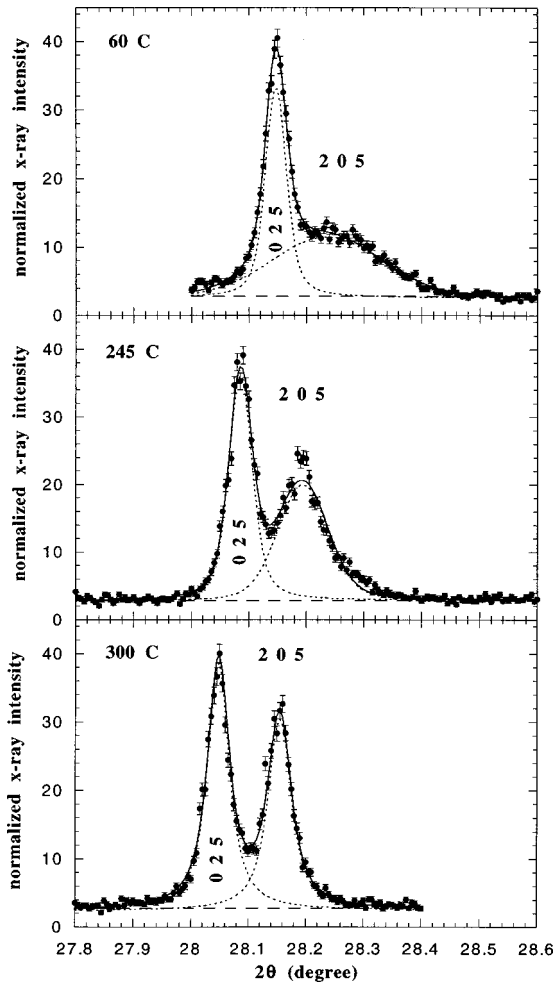


FIG. 5. Temperature-dependent x-ray-diffraction pattern of the 025 (lower lying) and 205 (higher lying) reflections. The lines corresponds to Voigtain fits.

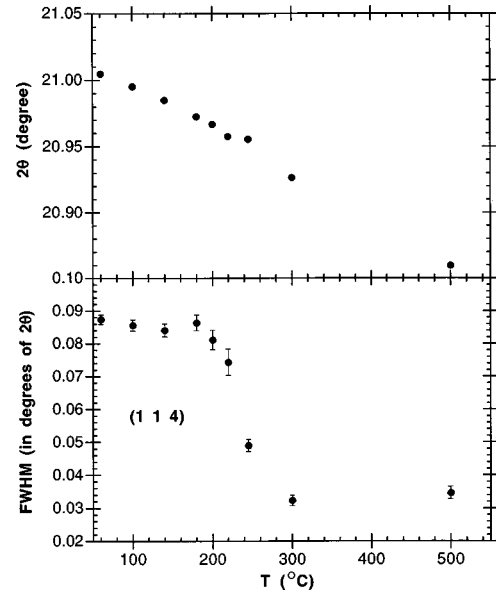


FIG. 6. Temperature dependence of the  $2\theta$  position (upper panel) and the full width at half maximum (FWHM) (lower panel) of the 114 reflection in  $\text{Pb}_2\text{Sr}_2\text{YCu}_3\text{O}_{8+\delta}$ .

constant below 180 °C it decreases around 220 °C and is again constant above 300 °C. In contrast to  $\Gamma$ , the position of the reflection does not exhibit any anomaly as a function of temperature, just the normal thermally induced shift, corresponding to a slight increase of the unit-cell volume with increasing temperature. Therefore, the drop in  $\Gamma$  is postulated to arise from a second-order phase transition between the disorder and the ordered (relaxed) state around 240 °C. The disorder-order transition lies in the temperature region where oxygen starts to be absorbed into the lattice when heated in an oxygen atmosphere (see Fig. 7). Therefore, this transition may be related to the ability of oxygen ions to hop between sites, in other words with oxygen diffusion in the sample.

#### IV. DISCUSSION AND CONCLUSIONS

Any model describing the selected line broadening must incorporate the fact that the variance in  $a$ ,  $b$ , and  $c$  are small (i.e.,  $S_{11}$ ,  $S_{22}$ , and  $S_{33}$ ), and that the dominant term in the

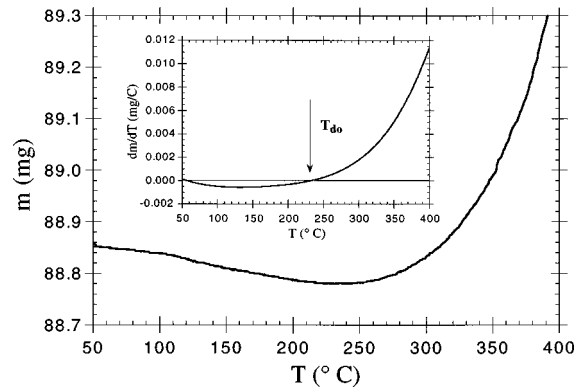


FIG. 7. Thermogravimetric analysis (TGA) plot for  $\text{Pb}_2\text{Sr}_2\text{YCu}_3\text{O}_{8+\delta}$ . Inset: Smoothed first derivative of the TGA plot. The zero crossing corresponds to the  $T_{do}$  transition temperature.

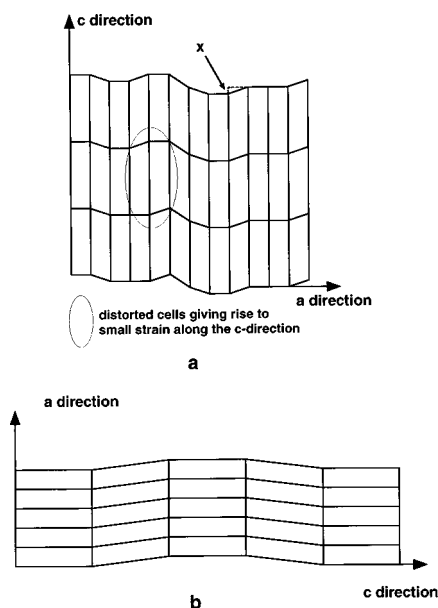


FIG. 8. (a) and (b) Schematic representations of the two models explained in the text describing the distortions of the unit cells in the  $(a, c)$  plane in the  $\text{Pb}_2\text{Sr}_2\text{Y}_{1-x}\text{Ca}_x\text{Cu}_3\text{O}_{8+\delta}$  structure.

covariance matrix is  $S_\beta$ . A well ordered lattice with a  $\beta$  angle different from  $90^\circ$  would result in a monoclinic unit cell. That we see an unresolvable broadening indicates that there is a random distribution of  $\beta$  angles around  $90^\circ$  with a correlation length smaller than that resolvable by x rays with  $\lambda = 1 \text{ \AA}$ . Two simple models, shown in Figs. 8(a) and 8(b), can be proposed that assume random distributions of the  $\beta$  angle, while maintaining a mean value of  $90^\circ$ . These models can explain the distribution of  $d$  spacings in the  $(a, c)$  plane.

The first model is based on a random modulation of the unit cells along the  $a$  direction with offsets along the  $c$  direction, which gives rise to deviations of the local bond angle from  $90^\circ$  [Fig. 8(a)]. Assuming an unchanged bond length of the very stiff Cu-O-Cu bonds, a random distribution of  $d$  spacings along the  $a$  direction would be induced too. Based on this model we can calculate the variance of the proposed offset  $x$  (see Fig. 8) of the unit cell along the  $c$  direction. The variance of the offset along the  $c$  direction is  $0.005 \text{ \AA}$ . The corresponding variance of the angle in the  $(a, c)$  plane is  $0.071^\circ$  ( $S_\beta$ ).

The second model is based on a random modulation of the

unit cells along the  $c$  direction with offsets along the  $a$  direction. Again the local angle in the  $a, c$  plane deviates from  $90^\circ$  (Fig. 8b). In this model, the length of the Cu-O-Cu bonds is preserved. Assuming that the face line of the cell is locally preserved, then the  $d$  spacings along the  $c$  direction would get slightly randomized. In contrast to the previous model, such a small random distribution along the  $c$  direction is observed ( $S_{33}$  term). However, this argument is certainly not strong enough for an unambiguous exclusion of the first model.

Whichever model is chosen, it is clear that these results are consistent with a distribution of  $\beta$  angles, and not with an unresolved monoclinic distortion. This finding argues against the proposed effect of oxygen doping, in which it is suggested that each unit cell has a stoichiometry of either  $\text{O}_8$  or  $\text{O}_9$ , and that these two phases form into domains of differing sizes.<sup>22</sup> In that case the broadening would correspond to resolvable monoclinic splittings. The exact defect mechanism that is causing the distribution of  $\beta$  angles is not understood but it is interesting to note that the  $(\text{Bi,Pb})_2\text{Sr}_2\text{CaCu}_2\text{O}_{8+\delta}$  compounds show similar distortions, although, there the distortions are ordered with an incommensurable modulation along the crystallographic  $b$  direction.<sup>4,5</sup> In addition, in the  $(\text{Bi,Pb})_2\text{Sr}_2(\text{Ca/Y})\text{Cu}_2\text{O}_{8+\delta}$  compounds the modulation depends strongly on the Bi to Pb ratio. The incommensurate modulation of the lattice is found to be smaller for Pb doped samples and vanishes for samples with about more than 40% Pb. We note that it is not possible to replace all the  $\text{Bi}^{3+}$  by  $\text{Pb}^{2+}$ , except when an additional  $\text{Cu}^{1+}$  plane is added to restore the charge equilibrium. This leads then to the very similar structure of the  $\text{Pb}_2\text{Sr}_2(\text{R/Ca})\text{Cu}_3\text{O}_{8+\delta}$  series under investigation here. Therefore, a continuous transformation between these two types of structures is not possible. However, our results in connection with the results on the  $(\text{Bi,Pb})_2\text{Sr}_2(\text{Ca/Y})\text{Cu}_2\text{O}_{8+\delta}$  found in the literature may lead to a more fundamental understanding of oxygen related disorder in these high- $T_c$  cuprates.

## ACKNOWLEDGMENTS

We would like to thank P. Fischer and M. Medarde (PSI) for helpful discussions. This work is partly supported (L.S. and S.S.) by the DOE-BES, Chemical Sciences, under Contract No. W-31-109-ENG-38. We are grateful to the Swiss-Norwegian Beamline Project for providing access to synchrotron radiation and suitable experimental facilities.

<sup>1</sup>E. F. Skelton, A. R. Drews, M. S. Osofsky, S. B. Qadri, J. Z. Hu, T. A. Vanderah, J. L. Peng, and R. L. Greene, *Science* **263**, 1416 (1994).

<sup>2</sup>T. Zeiske, R. Sonntag, D. Hohlwein, N. H. Andersen, and T. Wolf, *Nature (London)* **353**, 542 (1991).

<sup>3</sup>P. G. Radaelli, D. J. Jorgensen, A. J. Schultz, J. L. Peng, and R. L. Greene, *Phys. Rev. B* **49**, 15 322 (1994).

<sup>4</sup>H. W. Zandbergen, W. A. Groen, A. Smit, and G. Van Tendeloo, *Physica C* **168**, 426 (1990).

<sup>5</sup>A. Yamamoto, M. Onoda, E. Takayama-Muromachi, F. Izumi, T. Ishigaki, and H. Asano, *Phys. Rev. B* **42**, 4228 (1990).

<sup>6</sup>P. Berastegui, P. Fischer, I. Bryntse, L.-G. Johansson, and A. W. Hewat, *Solid State Chem.* **127**, 31 (1996).

<sup>7</sup>B. Roessli, P. Fischer, U. Staub, M. Zolliker, and A. Furrer, *Europhys. Lett.* **23**, 511 (1993).

<sup>8</sup>T. W. Clinton, J. W. Lynn, J. Z. Liu, Y. X. Jia-YX, T. J. Goodwin, R. N. Shelton, B. W. Lee, M. Buchgeister, M. B. Maple, and J. L. Peng, *Phys. Rev. B* **51**, 15 429 (1995).

<sup>9</sup>U. Staub, L. Soderholm, S. Skanthakumar, S. Rosenkranz, C. Ritter, and W. Kagunya, *Z. Phys. B* **104**, 37 (1997).

<sup>10</sup>L. Soderholm, S. Skanthakumar, U. Staub, Mark R. Antonio, and C. W. Williams, *J. Alloys Compd.* **250**, 623 (1997).

- <sup>11</sup>S. Skanthakumar and L. Soderholm, *Phys. Rev. B* **53**, 920 (1996).
- <sup>12</sup>U. Staub, L. Soderholm, S. Skanthakumar, and M. R. Antonio, *J. Phys. V* **7**, C2-1077 (1997).
- <sup>13</sup>U. Staub, L. Soderholm, S. Skanthakumar, and M. R. Antonio, *Phys. Rev. B* **52**, 9736 (1995).
- <sup>14</sup>U. Staub, L. Soderholm, S. Skanthakumar, R. Osborn, and F. Fauth, *Europhys. Lett.* **39**, 663 (1997).
- <sup>15</sup>L. F. Schneemeyer, J. V. Waszczak, S. M. Zahorak, R. B. Van Dover, and T. Siegrist, *Mater. Res. Bull.* **22**, 1467 (1987).
- <sup>16</sup>J. S. Xue, M. Reedyk, A. Dabbowski, H. Dabkowska, J. E. Greedan, and C. H. Chen, *J. Cryst. Growth* **113**, 371 (1991).
- <sup>17</sup>H. Fujishita, M. Sato, Y. Morii, and S. Funahashi, *Physica C* **210**, 529 (1993).
- <sup>18</sup>J. S. Xue, J. E. Greedan, and M. Maric, *J. Solid State Chem.* **102**, 501 (1993).
- <sup>19</sup>J. E. Jorgenson and N. H. Anderson, *Acta Chem. Scand.* **45**, 19 (1991).
- <sup>20</sup>R. J. Cava, M. Marezio, J. J. Krajewski, W. F. Peck, Jr., A. Santoro, and F. Beech, *Physica C* **157**, 272 (1989).
- <sup>21</sup>C. Chaillout, O. Chmaissem, J. J. Capponi, T. M. Fournier, G. J. McIntyre, and M. Marezio, *Physica C* **175**, 293 (1991).
- <sup>22</sup>M. Marezio, A. Santoro, J. J. Capponi, E. A. Hewat, R. J. Cava, and F. Beech, *Physica C* **169**, 401 (1990).
- <sup>23</sup>H. W. Zandbergen, K. Kadowaki, M. J. V. Menken, A. A. Menovsky, G. Van Tendeloo, and S. Amelinckx, *Physica C* **158**, 155 (1989).
- <sup>24</sup>E. A. Hewat, J. J. Capponi, R. J. Cava, C. Chaillout, M. Marezio, and J. L. Tholence, *Physica C* **157**, 509 (1989).
- <sup>25</sup>J. E. Jørgensen, *Solid State Commun.* **80**, 613 (1991).
- <sup>26</sup>J. Rodríguez-Carvajal, M. T. Fernández-Díaz, and J. L. Martínez, *J. Phys.: Condens. Matter* **3**, 3215 (1991).
- <sup>27</sup>J. Rodríguez-Carvajal, *Physica B* **192**, 55 (1993).